Synthesis, Characterisation and Electrochemical Behaviour of Rhodium(III) Complexes Containing 1,2-Naphthoquinone-2-oxime and Formation of Imine Complexes through N−O Bond Cleavage

Xiao-Xia Liu[a] and Wing-Tak Wong*[a]

Keywords: Rhodium / N ligands / Electrochemistry

The new rhodium(III) complexes [Rh(η^2-nqo)L_2Cl_2] **(1a–1d)** and [Rh(η^2-nqo)$_2$LCl] **(2b–2d)** [**1a**, L = PPh_3; **1b,2b**, L = pyridine (py); **1c,2c**, L = 4-phenylpyridine (ppy); **1d,2d**, L = 4-acetylpyridine (apy)] have been prepared by treatment of the reaction mixture of $RhCl_3{\cdot}3H_2O$ and 1,2-naphthoquinone-2-oxime (nqo) in ethanol by P or N donor ligands. Cyclic voltammetric studies show that the new complexes display an irreversible metal-localised two-electron reduction from Rh^{III} to Rh^{I}, accompanied by the loss of the chloride ligands. The 1,2-naphthoquinone-2-imine (nqi) complexes [Rh(η^2-nqo)(η^2-nqi)Cl_2]·L **(3b–3d)** (**3b**, L = py; **3c**, L = ppy; **3d**, L = apy), [Rh(η^2-nqo)(η^2-nqi)Cl_2] **(4)** and [Rh(η^2-nqo)$_2$(nqi)Cl] **(5)** were obtained by deoxygenation of the oxime group in which N–O bond cleavage is observed. The molecular structures of **1a**, **2b**, **4** and **5** were established by single crystal X-ray analyses.

Introduction

Rhodium(III) complexes containing chloride ligands have attracted much attention. They have been shown to be active in processes such as the photochemical[1] and the electrochemical[2−5] reduction of protons or water to dihydrogen, the electrocatalytic hydrogenation of organics,[2−4] and the electrochemical regeneration of NADH from NAD^+.[6,7] Most of the complexes mentioned above contain 2,2-bipyridine type ligands. 1,2-Naphthoquinone-monooximes are another kind of donor ligand with a π-accepting ability.[8,9] In ruthenium 1,2-naphthoquinone-1-oxime complexes, the MLCT from ruthenium(II) to the ligand occurs with comparatively low energy.[10] The existence and the number of this ligand in 2,2-bipyridine-containing ruthenium complexes influence the electrochemical property of the metal centre.[11] Metal complexes containing 1,2-naphthoquinone-monooximes are of interest as they are widely used for analytical purposes[12,13] and are potentially useful for the preparation of a wide variety of organic compounds.[14−17] However, most of the studies have been concerned with first-row transition metals.[14−20] Reports dealing with these ligands involving complexes of second-row transition metals are very limited.[9,11,21,22] As a continuation of our studies on 1,2-naphthoquinone-monooxime complexes of second row transition metals,[10,23−25] we herein present the formation of a series of chloro rhodium(III) complexes containing 1,2-naphthoquinone-2-oxime (abbreviated as nqoH).

Results and Discussion

Synthesis and Characterisation of Rhodium(III) Complexes [Rh(η^2-nqo)L_2Cl_2] (1a−1d) and [Rh(η^2-nqo)$_2$LCl] (2b−2d)

The new rhodium(III) complexes [Rh(η^2-nqo)L_2Cl_2] **(1a−1d)** and [Rh(η^2-nqo)$_2$LCl] **(2b−2d)** [**1a**, L = PPh_3; **1b,2b**, L = pyridine (py); **1c,2c**, L = 4-phenylpyridine (ppy); **1d,2d**, L = 4-acetylpyridine (apy)] were synthesised by the treatment of a reaction mixture of $RhCl_3{\cdot}3H_2O$ and 1,2-naphthoquinone-2-oxime in refluxing ethanol with PPh_3, pyridine, 4-phenylpyridine or 4-acetylpyridine (Scheme 1). Characterisation of the new complexes by spectroscopic methods (^{1}H NMR, FAB MS) reveals that **1a−1d** contain one nqo and two P or N donor ligands coordinated to the metal centre (Table 1). In order to establish the molecular structure of complex **1a**, a single-crystal X-ray diffraction analysis was carried out. The molecular structure of **1a** is depicted in Figure 1, while bond lengths and angles are available in the Supporting Information. The molecule of **1a** contains a pseudo octahedrally coordinated rhodium centre. The nqo ligand coordinates to the metal centre through its oximato N and naphthoquinonic O atoms to form a five-membered metallocyclic ring [O(1)−Rh−N(1) 81.3(2)°]. This coordination mode is very common for 1,2-naphthoquinone-monooxime ligands.[9,10,16,19−25] The molecule also contains two chloride atoms [Cl(1) and Cl(2)], which are *trans* to the oximato N and naphthoquinonic O atoms, respectively ([N(1)−Rh−Cl(1) 170.8(1)°], [O(1)−Rh−Cl(2) 176.5(1)°]), forming an equatorial plane with the nqo ligand. The two phosphane ligands occupy the perpendicular positions to complete the six coordination configuration of the Rh metal centre ([P(1)−Rh−P(2) 178.32(5)°]). The mean Rh−P distance is 2.3945(1)Å, which is similar to other Rh complexes with phosphane coordinated to their metal centre, such as in $[Rh(Hdmg)(bdio)(PEt_3)]^+[Rh(Hdmg)_2Cl_2]^-{\cdot}H_2O$ (dmg = dimethylglyoximato; bdio = 2,3-butanedione 2-imino 3-oxi-

---

[a] Department of Chemistry, The University of Hong Kong,
Pokfulam Road, Hong Kong
Fax: (internat.) +852-2547-2933, or -2857-1586
E-mail: wtwong@hkucc.hku.hk

💻 Supporting information for this article is available on the WWW under http://www.wiley-vch.de/home/eurjic or from the author.

1434−1948/01/0202−0511 $ 17.50+.50/0

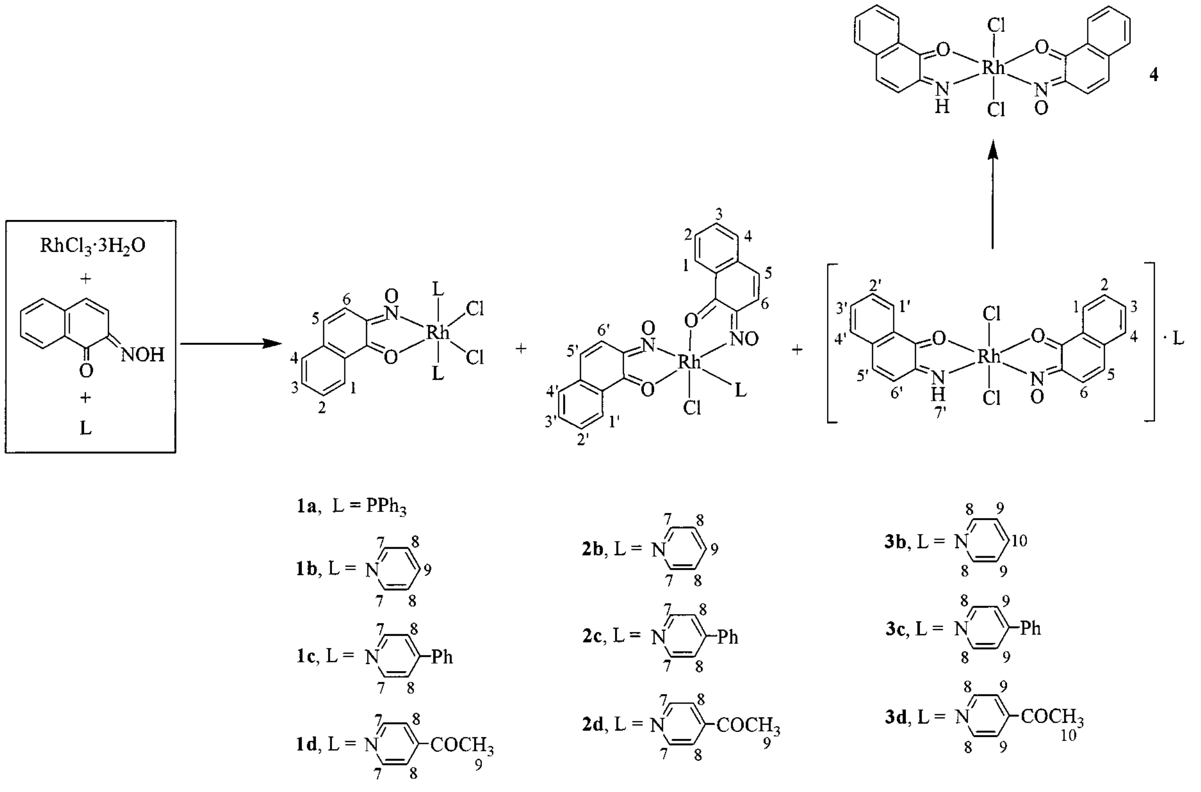

Scheme 1. Reaction of $RhCl_3·3H_2O$ with nqoH followed by treatment with the pyridyl ligand

mato), where the corresponding bond length is 2.3817(8)Å.[26] In the ^1H NMR spectra of the pyridine complexes **1b−1d**, the chemical shifts of the nqo proton signals are very similar to those in **1a**, showing that the nqo ligands have very similar chemical environments. Thus, complexes **1b−1d** are proposed to have similar molecular structures to **1a**, with the bidentate nqo ligand and the two chloride atoms occupying the equatorial plane, and the two pyridyl ligands occupying the perpendicular sites.

Characterisation of complexes **2b−2d** by spectroscopic methods (Table 1) reveals that they contain two nqo ligands, one pyridyl ligand and one chloride atom. A single crystal X-ray analysis was conducted on **2b**. The molecular structure of $[Rh(\eta^2\text{-nqo})_2(py)Cl]$ **(2b)** is depicted in Figure 2, while the bond parameters can be obtained from the Supporting Information. A distorted octahedral coordination of the rhodium metal centre is observed. The nqo ligands chelate to the metal centre in a similar way as in **1a** [O(1)−Rh−N(1) = 81.3(2)° and O(3)−Rh−N(2) 81.8(2)°]. The oximato N and the naphthoquinonic O atoms adopt a mutually *cis* geometry as in the ruthenium 1,2-naphthoquinone-2-oxime complexes *cis,cis*-$[Ru(\eta^2\text{-nqo})_2L_1L_2]$ (L_1, L_2 = CO or pyridyl ligands).[10,24] Pyridine is coordinated to the Rh centre through its N atom and is *trans* to the oximato N of an nqo ligand, as in *cis,cis*-$[Ru(\eta^2\text{-nqo})_2(CO)L]$ (L = pyridyl ligands).[10,24] The chloride atom is *trans* to the naphthoquinonic O atom of another nqo ligand, with a Rh−Cl bond length of 2.332(2)Å. This is consistent with the Rh−Cl distance in other rhodium complexes such as $[Rh(Hdmg)(bdio)(PEt_3)]^+[Rh(Hdmg)_2Cl_2]^-·H_2O$ [2.3320(9) Å].[26] The nqo ligands of **2b−2d** exist in a similar chemical environment, since they display very similar chemical shifts in their ^1H NMR spectra. The spatial arrangement of the ligands in complexes **2b−2d** should be the same. The asymmetry of the nqo ligands gives rise to the possibility for the presence of structural isomers other than **2b−2d**; in fact, we observe some other minor bands in the reaction mixture from TLC. Unfortunately, we could not isolate or characterise these compounds.

Electrochemistry of Complexes 1a−1d and 2b−2d

Cyclic voltammetry of complexes **1a−1d** and **2b−2d** was performed at a standard scan rate of 100 mV s^{-1} in CH_2Cl_2/0.1 M tetrabutylammonium hexafluorophosphate (TBAH). The redox potentials are listed in Table 2 and the representative cyclic voltammogram of **1a** is shown in Figure 3.

The electrochemical behaviour of $[Rh(\eta^2\text{-nqo})(PPh_3)_2Cl_2]$ **(1a)** resembles that of other chloro rhodium(III) complexes with 2,2′-bipyridyl ligands, such as $[RhL(P)_2(Cl)_2]^+$ [2,27] and $[RhL_2(Cl)_2]^+$,[3,28,29] and some complexes containing π-coordinated ligands $[Rh(C_5Me_5)LCl]^+$ (P = PPh_2Et or PPh_3; L = 2,2-bipyridyl ligands).[1,4−6,30−32] This behaviour is characterised by an irreversible, metal-localised two-electron reduction at peak potential E_{c1}, which is associated with the loss of the two chloride ligands (EC mechanism) yielding the Rh^I complex [Scheme 2, Equation (1)]. A controlled-potential electrolysis at a potential slightly negative to this wave, consumes two electrons per molecule of com-

Table 1. Spectroscopic data for compounds **1a−1d**, **2b−2d**, **3b−3d** and **4−7**

Complex	^{1}H NMR spectra (δ, *J*/Hz)	^{31}P NMR spectra (δ, *J*/Hz)	Mass spectra[a] (*m*/*z*)
1a	8.01 (d, *J* = 7.9, 1 H, H^{1}), 7.72−7.66 (m, phenyl, 12 H), 7.52 (m, 1 H, H^{3}), 7.37 (m, 1 H, H^{4}), 7.35 (m, 1 H, H^{2}), 7.30−7.25 (m, 6 H, phenyl), 7.22−7.17 (m, 12 H, phenyl), 6.48 (d, *J* = 9.5, 1 H, H^{5}), 6.32 (d, *J* = 9.5, 1 H, H^{6})[b]	18.26 [d, *J*(Rh,P) = 90.7]	834 (870)[c]
1b	8.99 (m, 2 H, H^{7}), 8.80 (m, 2 H, $H^{7'}$), 8.64 (m, 1 H, H^{1}), 7.98 (tt, *J* = 7.6, 1.5, 1 H, H^{9}), 7.90 (tt, *J* = 7.6, 1.5, 1 H, $H^{9'}$), 7.66 (m, 1 H, H^{3}), 7.60 (m, 1 H, H^{4}), 7.53 (m, 2 H, H^{8}), 7.51 (m, 1 H, H^{2}), 7.41 (m, 2 H, $H^{8'}$), 7.40 (d, *J* = 9.5, 1 H, H^{6}), 6.94 (d, *J* = 9.5, 1 H, H^{5})	−	504 (504)
1c	9.04 (br.d, *J* = 6.5, 2 H, H^{7}), 8.84 (m, 2 H, $H^{7'}$), 8.65 (d, *J* = 7.7, 1 H, H^{1}), 7.73 (m, 2 H, H^{8}), 7.74−7.68 (m, 4 H, phenyl), 7.67 (m, 1 H, H^{3}), 7.61 (m, 3 H, $H^{4,8'}$), 7.58−7.54 (m, 6 H, phenyl), 7.53 (m, 1 H, H^{2}), 7.42 (d, *J* = 9.5, 1 H, H^{6}), 6.95 (d, *J* = 9.5, 1 H, H^{5})[b]	−	621 (656)[c]
1d	9.19 (br.d, *J* = 6.6, 2 H, H^{7}), 9.00 (m, 2 H, $H^{7'}$), 8.61 (d, *J* = 7.9, 1 H, H^{1}), 7.95 (dd, *J* = 5.2, 2 H, 1.5, H^{8}), 7.82 (dd, *J* = 5.4, 2 H, 1.5, $H^{8'}$), 7.68 (m, 1 H, H^{3}), 7.61 (br.d, *J* = 7.2, 1 H, H^{4}), 7.52 (m, 1 H, H^{2}), 7.38 (d, *J* = 9.5, 1 H, H^{6}), 6.96 (d, *J* = 9.5, 1 H, H^{5}), 2.72 (s, 3 H, H^{9} or $H^{9'}$), 2.70 (s, 3 H, $H^{9'}$ or H^{9})	−	552 (588)[c]
2b	8.99 (br.d, *J* = 5.3, 2 H, H^{7}), 8.75 (d, *J* = 7.7, 1 H, H^{1}), 8.42 (d, *J* = 7.9, 1 H, $H^{1'}$), 7.89 (m, 1 H, H^{9}), 7.71 (m, 1 H, H^{3}), 7.63 (m, 1 H, $H^{3'}$), 7.62 (m, 1 H, H^{4}), 7.56 (m, 2 H, $H^{2,4'}$), 7.50 (m, 2 H, H^{8}), 7.42 (m, 1 H, $H^{2'}$), 7.33 (m, 1 H, $H^{6'}$), 7.18 (d, *J* = 9.5, 1 H, H^{6}), 6.90 (d, *J* = 9.5, 1 H, $H^{5'}$), 6.89 (d, *J* = 9.5, 1 H, H^{5})[b]	−	562 (562)
2c	8.99 (br.d, *J* = 6.6, 2 H, H^{7}), 8.77 (d, *J* = 8.0, 1 H, H^{1}), 8.44 (d, *J* = 7.8, 1 H, $H^{1'}$), 7.71 (m, 1 H, H^{3}), 7.67 (m, 2 H, H^{8}), 7.63 (m, 1 H, $H^{3'}$), 7.63−7.55 (m, 3 H, H^{4}, 2H of phenyl), 7.58 (m, 1 H, H^{2}), 7.52−7.49 (m, 4 H, $H^{4'}$, 3H of phenyl), 7.43 (m, 1 H, $H^{2'}$), 7.35 (d, *J* = 9.5, 1 H, $H^{6'}$), 7.20 (d, *J* = 9.5, 1 H, H^{6}), 6.91 (d, *J* = 9.5, 1 H, $H^{5'}$), 6.89 (d, *J* = 9.5, 1 H, H^{5})[b]	−	638 (638)
2d	9.20 (br.d, *J* = 6.5, 2 H, H^{7}), 8.73 (d, *J* = 7.9, 1 H, H^{1}), 8.41 (d, *J* = 8.4, 1 H, $H^{1'}$), 7.92 (dd, *J* = 5.1, 1.7, 2 H, H^{8}), 7.72 (m, 1 H, H^{3}), 7.63 (m, 1 H, $H^{3'}$), 7.62 (m, 1 H, H^{4}), 7.57 (m, 1 H, H^{2}), 7.56 (d, *J* = 7.8, 1 H, $H^{4'}$), 7.43 (m, 1 H, H^{2}), 7.31 (d, *J* = 9.5, 1 H, $H^{6'}$), 7.18 (d, *J* = 9.5, 1 H, H^{6}), 6.91 (d, *J* = 9.5, 1 H, $H^{5'}$), 6.89 (d, *J* = 9.5, 1 H, H^{5}), 2.64 (s, 3 H, H^{9})[b]	−	568 (604)[c]
3b	11.46 (br., 1 H, $H^{7'}$), 9.13 (m, 2 H, H^{8}), 8.64 (d, *J* = 8.1, 1 H, H^{1}), 8.24 (d, *J* = 7.6, 1 H, $H^{1'}$), 8.00 (t, *J* = 7.6, 1 H, H^{10}), 7.67 (m, 2 H, $H^{3,3'}$), 7.60 (m, 2 H, H^{9}), 7.57 (m, 1 H, H^{4}), 7.51 (m, 1 H, H^{2}), 7.48 (m, 1 H, $H^{2'}$), 7.39 (d, *J* = 9.5, 1 H, H^{6}), 7.32 (br.d, *J* = 7.6, 1 H, $H^{4'}$), 7.09 (br.d, *J* = 10.2, 1 H, $H^{6'}$), 6.96 (br.d, *J* = 10.2, 1 H, $H^{5'}$), 6.94 (d, *J* = 9.5, 1 H, H^{5})	−	582 (582)
3c	11.50 (br., 1 H, $H^{7'}$), 9.13 (br.d, *J* = 6.6, 2 H, H^{8}), 8.66 (d, *J* = 7.9, 1 H, H^{1}), 8.25 (d, *J* = 7.6, 1 H, $H^{1'}$), 7.77 (br.d, *J* = 6.6, 1 H, H^{9}), 7.75−7.72 (m, 2 H, phenyl), 7.67 (m, H, $H^{3'}$), 7.65 (m, 1 H, H^{3}), 7.61 (br.d, *J* = 7.1, 1 H, H^{4}), 7.58−7.54 (m, 3 H, phenyl), 7.51 (m, 1 H, H^{2}), 7.49 (m, 1 H, $H^{2'}$), 7.40 (d, *J* = 9.5, 1 H, H^{6}), 7.32 (br.d, *J* = 7.5, 1 H, $H^{4'}$), 7.11 (br.d, *J* = 10.2, 1 H, $H^{6'}$), 7.03 (br.d, *J* = 10.2, 1 H, $H^{5'}$), 6.95 (d, *J* = 9.5, 1 H, H^{5})[b]	−	658 (658)
3d	11.40 (br., 1 H, $H^{7'}$), 9.34 (br.d, *J* = 6.5, 2 H, H^{8}), 8.61 (d, *J* = 7.9, 1 H, H^{1}), 8.25 (d, *J* = 7.8, 1 H, $H^{1'}$), 7.99 (dd, *J* = 5.2, 1.5, 1 H, H^{9}), 7.68 (m, 1 H, $H^{3'}$), 7.66 (m, 1 H, H^{3}), 7.61 (br.d, *J* = 7.1, 1 H, H^{4}), 7.52 (m, 1 H, H^{2}), 7.49 (m, 1 H, $H^{2'}$), 7.38 (d, *J* = 9.5, 1 H, H^{6}), 7.33 (br.d, *J* = 7.4, 1 H, $H^{4'}$), 7.11 (dd, *J* = 10.1, 1.3, 1 H, $H^{6'}$), 6.98 (br.d, *J* = 10.1, 1 H, $H^{5'}$), 6.96 (d, *J* = 9.5, 1 H, H^{5}), 2.71 (s, 3 H, H^{10})[b]	−	624 (624)
4	−	−	331 (503)[d]
5	10.30 (br., 1 H, $H^{7''}$), 8.82 (d, *J* = 7.9, 2 H, $H^{1,1'}$), 7.98 (d, *J* = 7.4, 1 H, $H^{1''}$), 7.75 (br.d, *J* = 10.1, 1 H, $H^{5''}$), 7.67 (m, 1 H, H^{3} or $H^{3'}$), 7.65 (m, 1 H, $H^{3'}$ or H^{3}), 7.60 (m, 1 H, $H^{3''}$), 7.57 (m, 2 H, $H^{2,2'}$), 7.56 (br.d, *J* = 7.2, 2 H, $H^{4,4'}$), 7.39 (m, 1 H, $H^{6''}$), 7.37 (m, 1 H, $H^{2''}$), 7.34 (d, *J* = 9.5, 2 H, $H^{6,6'}$), 7.30 (br.d, *J* = 7.7, 1 H, $H^{4''}$) 6.86 (d, *J* = 9.5, 2 H, $H^{5,5'}$)	−	639 (640)
6	8.58 (d, *J* = 8.0, 3 H, $H^{1,1',1''}$), 7.69 (m, 3 H, $H^{3,3',3''}$), 7.60 (br.d, *J* = 7.4, 3 H, $H^{4,4',4''}$), 7.49 (m, 3 H, $H^{2,2',2''}$), 7.20 (d, *J* = 9.5, 3 H, $H^{6,6',6''}$), 6.92 (d, *J* = 9.5, 3 H, $H^{5,5',5''}$)[b]	−	620 (619)[e]
7	8.59 (d, *J* = 8.0, 1 H, H^{1}), 8.50 (d, *J* = 8.0, 2 H, $H^{1',1''}$), 7.70−7.64 (m, 3 H, $H^{3,3',3''}$), 7.60−7.57 (m, 3 H, $H^{4,4',4''}$), 7.51−7.45 (m, 3 H, $H^{2,2',2''}$), 7.27 (m, 1 H, H^{6} or $H^{6'}$ or $H^{6''}$), 7.25 (m, 1 H, H^{6} or $H^{6''}$), 7.20 (d, *J* = 9.5, 1 H, H^{6}, or $H^{6'}$ or $H^{6''}$), 6.95 (d, *J* = 9.5, 1 H, $H^{5'}$ or $H^{5''}$), 6.93 (d, *J* = 9.5, 2 H, $H^{5,5' or 5''}$)[b]	−	620 (619)[e]

[a] Calculated values in parentheses. − [b] By ^{1}H,^{1}H COSY NMR spectroscopy. − [c] Only $[M - Cl]^{+}$ is observed. − [d] Only $[M - nqo]^{+}$ is observed. − [e] By ESI MS.

plex and leads to a purple-coloured solution. We failed to isolate the purple product as it was not stable enough under our experimental conditions. The colour of the solution slowly changed to red on removing the applied potential. The reverse process, the reoxidation of the Rh^{I} complex, is also a two-electron step (E_{a1}), with subsequent completion of the coordination sphere of the d^{6} metal centre by addition of the chloride ligands [Equation (2)].

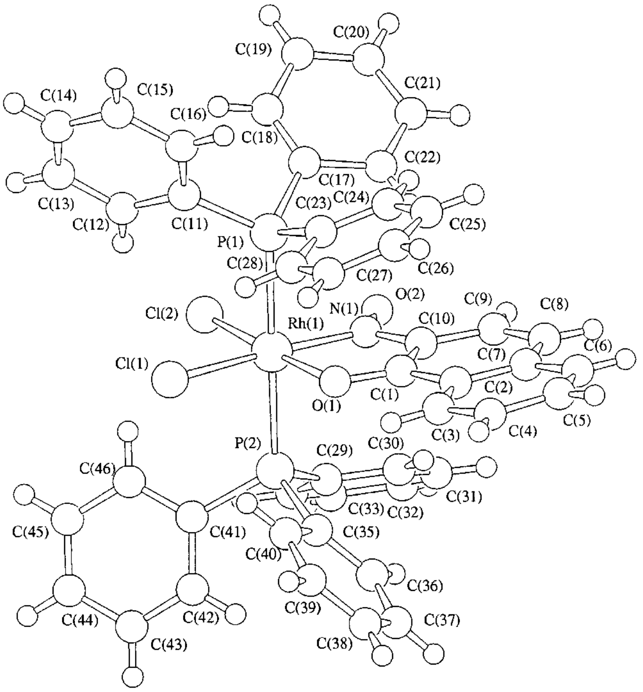

Figure 1. The molecular structure of [Rh(η^2-nqo)(PPh_3)$_2$$Cl_2$] **(1a)** with the atom numbering scheme

The Rh^I complex can be further reduced at a more negative potential with an apparently reversible (E_{c2}, E_{a2}) single-electron step. The 2,2-bipyridyl complexes displayed similar reversible redox couples, which have been attributed to the reduction of the pyridyl ligand, leading to the coordinated radical anion $L^{\cdot -}$. Lund reported the cyclic voltammetric study of fluorenone oxime (F1=NOH), which displayed a nearly reversible reduction at −1.67 V vs. SCE to its radical anion F1=$NOH^{\cdot -}$.[33] The reduction of the oxime group in a copper(II) complex [Cu(H_2L)(H_2O)$_2$]Cl_2 [L is a tripodal ligand containing an oxime group, such as *N*,*N*-(2-hydroxyacetophenyl)-(3-butane-2-oxime)-*N′*-(2-hydroxyacetophenyl)-1,2-diaminoethane] appeared around −1.5 V vs. SCE.[34] Similarly, the one-electron reduction of our nqo complex **1a** is oximato-ligand centred [Equation (3)] and leads to the radical anion. Compared with the free ligand (Table 2), the coordinated nqo is more difficult to reduce due to the π back-donation from the metal centre to the ligand.[30,35] This reduction process for complexes **1b**−**1d** appears at a more negative potential than that of **1a**. As the phosphane is a π-acceptor ligand, the degree of metal-to-nqo-ligand electron shift is smaller in **1a** than in **1b**−**1d**. This ligand-based reduction in complexes **1b**−**1d** is irreversible, and the reoxidation peak of Rh^I to Rh^{III} is not detected. In complexes **2b**−**2d**, apart from the irreversible metal-centred processes, two *quasi*-reversible one-electron reductions of the nqo ligands (E_{c2} for one nqo and E_{c3} for another) at less-negative potentials are observed. Since there are two nqo ligands in each of the **2b**−**2d** complexes,

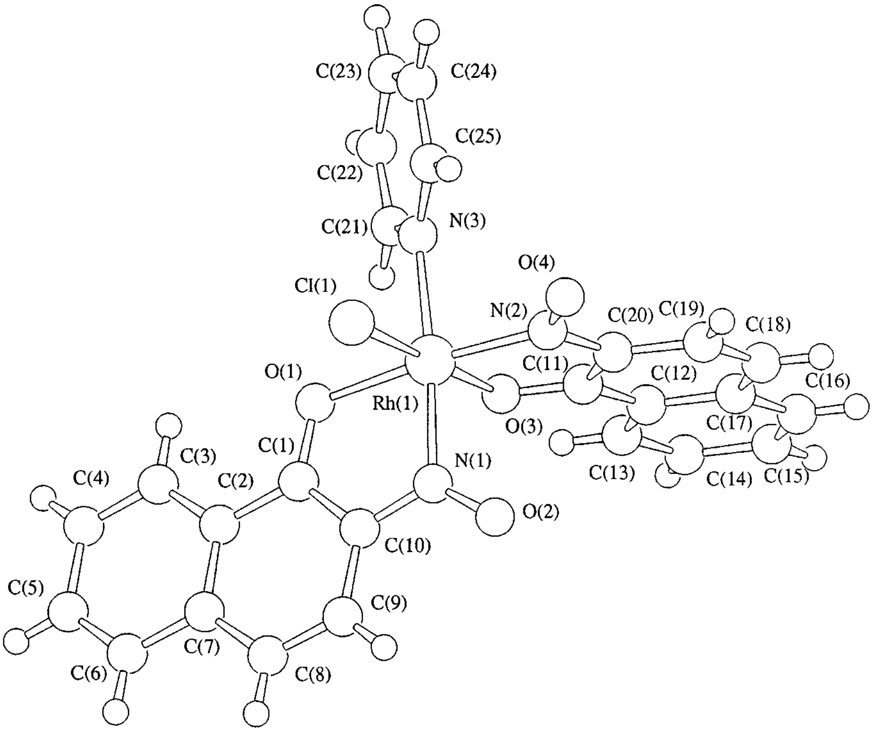

Figure 2. The molecular structure of [Rh(η^2-nqo)$_2$(py)Cl] **(2b)** with the atom numbering scheme

Table 2. Electrochemical data for the free ligand nqoH and complexes **1a−1d** and **2b−2d**

Compound	E_{c1} [a]	E_{a1}	E_{c2}	E_{a2}	$E_{a2}-E_{c2}$	E_{c3}	E_{a3}	$E_{a3}-E_{c3}$
nqoH	–	–	−1.08[b]	−0.87	0.21	–	–	–
1a	−1.23[b]	0.14	−1.61[c]	−1.51	0.10	–	–	–
1b	−1.12[b]	–	−1.81[b]	–	–	–	–	–
1c	−1.18[b]	–	−1.83[b]	–	–	–	–	–
1d	−1.19[b]	–	−1.81[b]	–	–	–	–	–
2b	−1.09[b]	−0.78	−1.26[d]	−1.15	0.11	−1.43[d]	−1.31	0.12
2c	−1.14[b]	−0.75	−1.31[d]	−1.15	0.16	−1.52[d]	−1.34	0.18
2d	−1.11[b]	−0.72	−1.23[d]	−1.12	0.11	−1.49[d]	−1.32	0.17

[a] Peak potentials in volts vs. $Fc^{0/+}$obtained from cyclic voltammetry at 100 mV s^{-1} in CH_2Cl_2/0.1 mol dm^{-3} TBAH. − [b] Irreversible. − [c] Apparently reversible. − [d] *Quasi*-reversible.

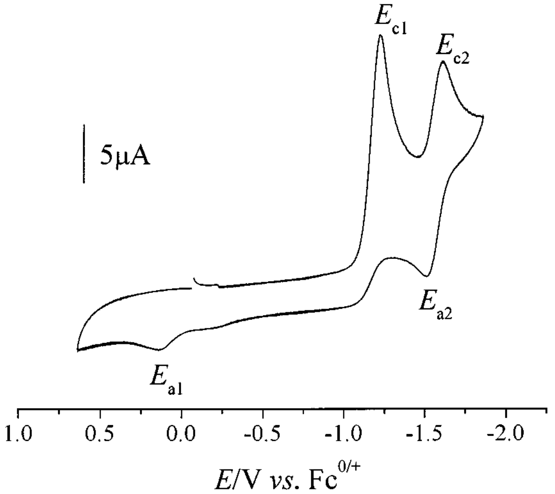

Figure 3. Cyclic voltammogram of $[Rh(\eta^2\text{-nqo})(PPh_3)_2Cl_2]$ **(1a)** in CH_2Cl_2 containing 0.1 mol dm^{-3} TBAH; scan rate, 100 mV s^{-1}

$$[Rh^{III}(nqo)(PPh_3)_2Cl_2] + 2e^- \xrightarrow{E_1} [Rh^{I}(nqo)(PPh_3)_2] + 2Cl^- \qquad (1)$$

$$[Rh^{I}(nqo)(PPh_3)_2] - 2e^- + 2Cl^- \xrightarrow{E_2} [Rh^{III}(nqo)(PPh_3)_2Cl_2] \qquad (2)$$

$$[Rh^{I}(nqo)(PPh_3)_2] + e^- \underset{E_4}{\overset{E_3}{\rightleftharpoons}} [Rh^{I}(nqo^{\cdot -})(PPh_3)_2]^- \qquad (3)$$

Scheme 2. Electrochemical reactions of $[Rh(\eta^2\text{-nqo})(PPh_3)_2Cl_2]$ **1a**

the π back-donation from the metal centre to each nqo ligand will be less than that in complexes **1b−1d** with only one nqo ligand present.

Formation of 1,2-Naphthoquinone-2-imine Complexes

The orange-red complexes **3b−3d** are also afforded in the reactions with pyridyl ligands (Scheme 1). Their ^1H NMR spectra show the signals for the naphthalene ring and pyridyl protons with an integration ratio of 2:1, and also a broad peak near δ = 11.4, assigned to the NH proton, which disappears after D_2O exchange. In the $^1H,^1H$ COSY spectra of **3c** and **3d**, this peak is coupled with proton $H^{6'}$of the nqo-derived ring. It can be assigned to the proton on the imino N atom. Slow evaporation of a $CHCl_3$ solution of complexes **3b−3d** gave a red crystalline product **4**. An X-ray diffraction analysis was carried out on a single crystal to elucidate the molecular structure. The molecular structure of **4** is shown in Figure 4, and the corresponding bond parameters are available from the supplementary material. The molecule contains two chloride atoms, one nqo ligand and one oximato deoxygenated nqo ligand. There is no pyridyl ligand. The central metal atom also adopts a distorted octahedral coordination mode, as in **1a** and **2b**. The two chloride atoms are *trans* to each other [Cl(1)−Rh−Cl(2) = 178.5(2)°] and the two naphthalene-derived rings occupy the equatorial plane. The nqo and the nqo-derived ligands adopt a chelate mode to the metal centre. The C−O bond length O(3)−C(11) in the nqo-derived ligand is 1.24(2)Å, which is comparable with the corresponding bond length for the quinonic group [C−O = 1.247(5)Å] in 3-hydroxy-2-methyl-1,4-benzoquinone 4-oxime,[36] and is smaller than the corresponding one [O(1)−C(1) = 1.32(1)Å] for the nqo ligand in the same molecule. The C−N bond length ([N(2)−C(20) = 1.27(1) Å]) is of a similar length to the imino C−N bond length [1.294(5)Å] in $[Rh(Hdmg)(bdio)(PEt_3)_2]^+[Rh(Hdmg)_2Cl_2]^-\cdot H_2O$[26] and also to that in $[TcCl(dmg)_2(bdio)BEt]$ [av. C−N = 1.29(1)Å].[37] This bond length is shorter than the corresponding one [N(1)−C(10) = 1.43(2)Å] for the nqo ligand, similar to the situation for the naphthoquinonic group. Complex **4** can be obtained from all three orange-red complexes **3b−3d** (based on X-ray single crystal analyses and FAB MS data) under very mild conditions (prolonged standing in $CHCl_3$ solution at room temperature for one day or at −20 °C for a few days). In addition, the pyridyl ligands in **3b−3d** can be exchanged with one another, provided that an excess of the pyridyl ligand of the desired complex is added (see below). We suggest that **3b−3d** are formed through interaction of the pyridyl ligands with part of a surrounding ligand in **4**. The nqo ligand is believed to undergo N−O bond cleavage of the oximato moiety to give the 1,2-naphthoquinone-2-imino (nqi) ligand, and complex **4** can be formulated as $[Rh(\eta^2\text{-nqo})(\eta^2\text{-nqi})Cl_2]$. Unfortunately, due to the extremely low solubility of **4** in common solvents, we failed to get satisfactory ^1H NMR spectroscopic data. The MS data of **3b−3d** conform to the stoichiometry of a molecule containing two chloride atoms, one nqo ligand, one nqi ligand and a pyridine or derived ligand. These complexes can be formulated as $[Rh(\eta^2\text{-nqo})(\eta^2\text{-nqi})Cl_2]\cdot L$ (**3b**, L = py; **3c**, L = ppy; **3d**, L = apy).

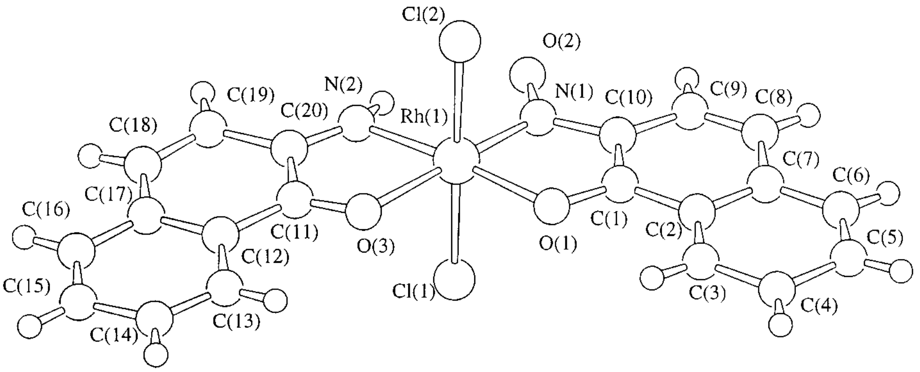

Figure 4. The molecular structure of [Rh(η^2-nqo)(η^2-nqi)Cl_2] **(4)** with the atom numbering scheme

Conversion Among 3b−3d Through Pyridyl Ligand Exchange

Pyridyl ligand exchange of **3d** by a tenfold excess of pyridine or 4-phenylpyridine at 30 °C was conducted in $CDCl_3$. The reaction mixture was continuously monitored by ^1H NMR spectroscopy and a change in the spectrum observed after 1 h. The proton resonances due to **3d** gradually decrease, accompanied by an increase in the intensities of other proton signals. The proton resonances of **3d** completely disappear after one day. A single product **3b** or **3c** is formed in the two reaction mixtures. The identity of **3b** and **3c** are confirmed by both ^1H NMR spectroscopy and their chromatographic properties. Pyridyl ligand exchange of **3b** by a tenfold excess of 4-acetylpyridine similarly gives **3d** after one day at 30 °C. No crystals of **4** are obtained in these reaction mixtures, even when they stand at room temperature for a long time. This ligand-exchange reaction rate is found to be sensitive to the amount of pyridyl ligand added. A substantial increase in the amount of ligand added results in a faster ligand exchange. This result, along with the isolation of **4** from the $CHCl_3$ solution of **3b−3d**, supports the hypothesis that **3b−3d** are adducts of **4** and the corresponding pyridyl ligand through comparatively loose interaction.

Other Routes for N−O Bond Cleavage of the Oxime Group in 1,2-Naphthoquinone-2-oxime and the Formation of Tris(1,2-naphthoquinone-2-oximato)rhodium(III) Complexes

A low yield (10%) of the N−O bond cleavage product [Rh(η^2-nqo)$_2$(nqi)Cl] **(5)** was obtained from the reaction of nqoH with [Rh^I(μ-Cl)$(CO)_2$]$_2$ in benzene. The reaction also affords the tris(1,2-naphthoquinone-2-oximato)-rhodium(III) complexes, *fac*-[Rh(η^2-nqo)$_3$] **(6)** in a 40% yield and *mer*-[Rh(η^2-nqo)$_3$] **(7)** in a 10% yield (Scheme 3). The molecular structure of complex **5** was confirmed by X-ray single crystal analysis. The structure of **5** is shown in Figure 5, while the bond parameters are available from the Supporting Information. The central metal atom adopts an essentially octahedral geometry with three naphthalene-derived rings and one chloride atom. Two of the naphthalene rings are nqo ligands, which occupy the equatorial plane and chelate to the Rh centre in a similar way to other nqoH complexes[10,20,24] including **1a**, **2b** and **4**. The oximato groups, as well as the naphthoquinonic O atoms, adopt a *cis* geometry relative to each other. This differs from our previously determined ruthenium complex *trans,trans*-[Ru{η^2-(1-nqo)}$_2$$(PBu_3)_2$] (1-nqo = 1,2-naphthoquinone-1-oximato), where both of the oximato N and the naphthoquinonic O atoms in the two equatorial 1-nqo ligands adopt a mutual *trans* geometry.[10] One of the perpendicular positions in **5** is occupied by a chloride atom and the other by an imino N atom of the 1,2-naphthoquinone-2-imino ligand, obtained through the deoxygenation of the oxime group in 1,2-naphthoquinone-2-oxime. The naphthoquinonic O atom of nqi is left pendant with a C−O bond length of 1.26(2)Å, which is comparable with the corresponding ones in complex **4** [1.24(2)Å] and 3-hydroxy-2-

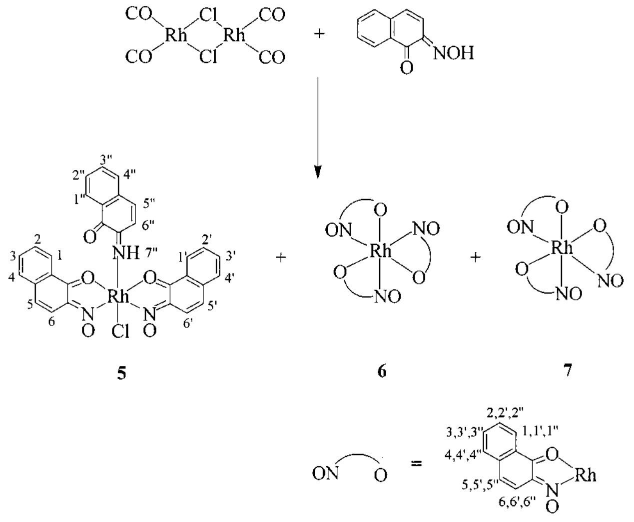

Scheme 3. Reaction of [Rh^I(μ-Cl)$(CO)_2$]$_2$ and nqoH

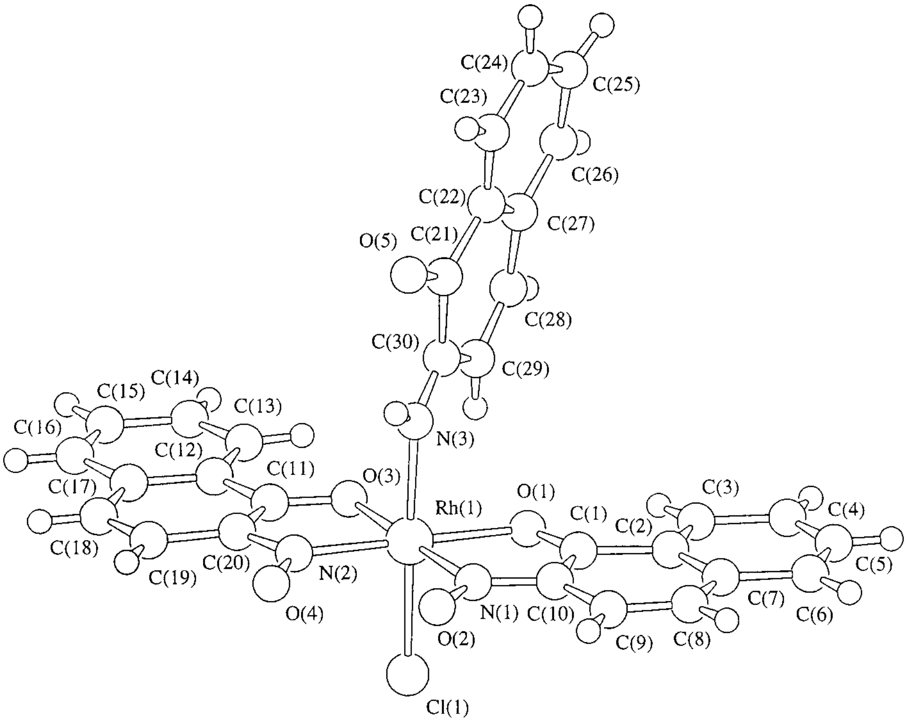

Figure 5. The molecular structure of [Rh(η^2-nqo)$_2$(nqi)Cl] **(5)** with the atom numbering scheme

methyl-1,4-benzoquinone-4-oxime [1.247(5)Å].[36] The C−N bond length of the nqi ligand is [N(3)−C(30) = 1.26(2)Å], which is in good agreement with that in the imino group [N(2)−C(20) = 1.27(1)Å] in **4**. The proton of the NH group appears as a broad peak at $\delta = 10.30$ in the ^{1}H NMR spectrum (Table 1) and also disappears after D_2O exchange.

Previously, there were two other reports on the reduction of the oxime group to imine in rhodium complexes.[26,38] In both cases, $NaBH_4$ was used as the reducing agent. [Rh^{III}(Hdmg)(H$_2$dmg)Cl$_2$][26] was first reduced to the Rh^I complex and, upon addition of phosphanes of small size and good donor ability, Rh^I was reoxidised to Rh^{III}, accompanied by the reduction of one of the equatorial oxime groups to imine. We have demonstrated a ruthenium carbonyl-induced deoxygenation of 1,2-naphthoquinone-1-oxime, leading to a coordinated 1,2-naphthoquinone-1-imine intermediate.[23] The ruthenium cluster with naphthoquinone-imino ligands was obtained in low yield through the following coupling reaction. The formation of 1,2-naphthoquinone-2-imine in complex **5** may be caused by the reduction of the oxime group by Rh^I to imine, which is stabilised towards hydrolysis by coordination to the Rh^{III} metal centre. However, in the reaction with $RhCl_3 \cdot 3H_2O$ as the starting material and in the presence of pyridine-type ligands, we have no reducing agent in the system. There are some other reports on the metal-induced deoxygenation of 1,2-naphthoquinone-mono-oxime,[14−18] however, they are all concerned with first-row transition metals. Treatment of the 1,2-naphthoquinone-2-oxime copper(II) complex with PPh_3 gave 2-amino-*N*^{4}-(1-hydroxy-2-naphthyl)-1,4-naphthoquinone 4-imine,[16] while 2-amino-1,4-naphthoquinone 4-*N*-phenylimine was obtained on treatment with aniline.[17] Both indicated the formation of nitrene/quinone imine intermediates obtained through the deoxygenation of the oximato group of the ligand. Direct evidence for the imine formation was given by the imine complexes [Fe(qo−A)$_2$] (where qo−A = 4-phenylamino-1,2-naphthoquinone-mono-imine) obtained through the interaction of pentacarbonyl iron(0) with 1,2-naphthoquinone-mono-oxime in the presence of aniline.[18] The reaction between [Cu{η^2-(1-nqo)}$_2$] and aniline gave an imine complex, bis(4-phenylimino-1,2-naphthoquinone-1-imino)bis(aniline)copper(II).[17] The mechanism for the formation of the nqi ligand in **3b**−**3d** and **4** is not certain at this point; however, we believe it occurs as a result of the modification of the coordinated nqo ligand as in the Cu^{II} analogue.[17]

The molecular formulae of **6** and **7**, as established by electrospray ionisation (ESI) mass spectrometry, are consistent with the calculated experimental isotopic patterns for $C_{30}H_{18}N_3O_6Rh$, and reveal their isomeric nature. The isomerism of **6** and **7** was confirmed by ^{1}H NMR spectroscopy in $CDCl_3$. Complex **6** gives rise to the same ^{1}H NMR signals for the three ligands showing that it has a highly symmetrical *fac* geometry as in a very recently structurally characterised ruthenium 1-nqo analogue [Ru{η^2-(1-nqo)}$_3$]$^-$, in which only one set of 1-nqo signals is present for the three ligands.[22] A nickel complex anion [Ni(4-Clqo)$_3$]$^-$ (4-Clqo = 4-chloro-1,2-benzoquninone-2-oximato)[39] and a naturally occurring pigment ferroverdin[40] *fac*-[Fe^{II}{4-[*p*-($CH_2{=}CH$)$C_6H_4OC({=}O)$]-1,2-benzoquninone-2-oximato}$_3$]$^-$ are other examples of *fac* geometry based on X-ray evidence. Although without X-ray analysis, the geometry of [Fe^{II}(RQ)$_3$]$^-$ (RQ = 4-R-1,2-benzoquninone-2-oximato, R = Me, *t*Bu, Cl, Br[41] and 3,4-benzo[42]) were also deduced to be *fac*, since the three ligands in the molecule are equivalent (shown by ^{1}H NMR spectroscopy). The three naphthalene rings of complex **7** give rise to different ^{1}H NMR signals, although some of them merge together to give intensified peaks. Thus, complex **7** is proposed to have *mer* geometry as in $[\mathrm{Mn^{III}L_3}]$ (L = 4-chloro-1,2-benzoquinone-2-oximato)[43] and $[\mathrm{Ni^{III}(RQ)_3}]$ (RQ = 4-R-1,2-benzoquininone-2-oximato, R = Me, *t*Bu and Cl).[44] However, when $[\mathrm{Mn^{III}L_3}]$ is electrochemically reduced to anionic $[\mathrm{Mn^{II}L_3}]^-$, it exists as a mixture of *fac* and *mer* isomers, both in solution (by ^{1}H NMR spectroscopy) and in the solid state (by X-ray analysis).[43] It was suggested that the favourable *mer* geometry for neutral complexes is partially due to a steric factor, the pendant oximato oxygen atoms are further apart than in the *fac* form. The origin of the *fac* form could be the effect of electrostatic stabilisation.[44] Nevertheless, the complexes are neutral in our system, the *fac* isomer is very favourable and there is no isomerisation observed after separation. This *fac* geometry is also favoured in the tris(arylazooximato)rhodium(III) complexes,[45] whereas the cobalt(III) analogues[46] exist exclusively in the *mer* form. This was explained by an increase in the facial area in going from the Co$^{\mathrm{III}}$ to the Rh$^{\mathrm{III}}$ chelate.[45]

Experimental Section

All manipulations were carried out under nitrogen with standard Schlenk techniques. Chemicals were purchased from commercial sources and used as received. Preparative thin-layer chromatographic (TLC) plates were prepared from silica (Merck Kieselgel 60 GF$_{254}$). − ^{1}H NMR spectra were obtained on a Bruker DPX-300 spectrometer using deuterated chloroform as the lock and reference. − Fast atom bombardment (FAB) mass spectra were recorded on a Finnigan MAT 95 mass spectrometer. Electrospray ionisation quadropole ion trap mass spectra were obtained on a Finnigan LCQ$^{\mathrm{TM}}$ LC/MS$^{\mathrm{n}}$ system. − Electrochemical measurements were conducted on a PAR 273A potentiostat in CH_2Cl_2 containing 0.1 mol dm^{-3} *n*-tetrabutylammonium hexafluorophosphate (TBAH), using a conventional argon gas sealed three-electrode cell. The working electrode was a glassy carbon disc for cyclic voltammetry and a carbon plate for large-scale electrolysis. Potentials are reported vs. ferrocene internal standard (Fc$^{0/+}$).

Synthesis of $[\mathrm{Rh(\eta^2\text{-}nqo)(PPh_3)_2Cl_2}]$ (1a): Solid samples of $RhCl_3{\cdot}3H_2O$ (53 mg, 0.2 mmol) and 1,2-naphthoquinone-2-oxime (69 mg, 0.4 mmol) were dissolved in 100 mL ethanol and refluxed for 2 h. PPh_3 (105 mg, 0.4 mmol) in hot ethanol was then added and the solution refluxed for another 10 h. The solvent was then removed and the residue chromatographed by TLC, with a solvent mixture of *n*-hexane/CH_2Cl_2 (1:4, v/v) as the eluent to afford the complex $[\mathrm{Rh(\eta^2\text{-}nqo)(PPh_3)_2Cl_2}]$ (**1a**; 80%, 139 mg). Red crystals of **1a** were grown by slow evaporation of an *n*-hexane/$CHCl_3$ solution at room temperature. $C_{46}H_{36}Cl_2NO_2P_2Rh$ (870.56): calcd. C 63.5, H 4.2, N 1.6; found C 63.2, H 4.5, N 1.5.).

Synthesis of $[\mathrm{Rh(\eta^2\text{-}nqo)L_2Cl_2}]$ (1b−1d), $[\mathrm{Rh(\eta^2\text{-}nqo)_2LCl}]$ (2b−2d), $[\mathrm{Rh(\eta^2\text{-}nqo)(\eta^2\text{-}nqi)Cl_2}]{\cdot}\mathrm{L}$ (3b−3d) and the Formation of $[\mathrm{Rh(\eta^2\text{-}nqo)(\eta^2\text{-}nqi)Cl_2}]$ (4): A procedure analogous to the above was followed, adding pyridine (py), 4-phenylpyridine (ppy) or 4-acetylpyridine (apy), respectively, instead of PPh_3. Upon TLC separation with a solvent mixture of *n*-hexane/CH_2Cl_2 (1:5−1:6, v/v), the complexes $[\mathrm{Rh(\eta^2\text{-}nqo)L_2Cl_2}]$ **(1b−1d)**, $[\mathrm{Rh(\eta^2\text{-}nqo)_2LCl}]$ **(2b−2d)** and $[\mathrm{Rh(\eta^2\text{-}nqo)(\eta^2\text{-}nqi)Cl_2}]{\cdot}\mathrm{L}$ **(3b−3d)** (**1b−3b**, L = py; **1c−3c**, L = ppy; **1d−3d**, L = apy) were isolated. Upon standing in a $CHCl_3$ solution of **3b−3d** at room temperature for one day, red crystals of $[\mathrm{Rh(\eta^2\text{-}nqo)(\eta^2\text{-}nqi)Cl_2}]$ **4** were obtained. Red crystals of **2b** were grown by slow evaporation of *n*-hexane/$CHCl_3$ solution at −20 °C.
1b: $C_{20}H_{16}Cl_2N_3O_2Rh$ (504.1805): calcd. C 47.6, H 3.2, N 8.3; found C 47.8, H 3.1, N 8.1.
1c: $C_{32}H_{24}Cl_2N_3O_2Rh$ (656.3757): calcd. C 58.6, H 3.7, N 6.4; found C 58.3, H 3.9, N 6.3.
1d: $C_{24}H_{20}Cl_2N_3O_4Rh$ (588.2541): calcd. C 49.0, H 3.4, N 7.1; found C 48.7, H 3.2, N 7.3.
2b: $C_{25}H_{17}ClN_3O_4Rh$ (561.7884): calcd. C 53.4, H 3.1, N 7.5; found C 53.5, H 2.9, N 7.2.
2c: $C_{31}H_{21}ClN_3O_4Rh$ (637.8860): calcd. C 58.4, H 3.3, N 6.6; found C 58.7, H 3.4, N 6.4.
2d: $C_{27}H_{19}ClN_3O_5Rh$ (603.8252): calcd. C 53.7, H 3.2, N 7.0; found C, 53.6, H 2.9, N 7.2.
3b: $C_{25}H_{18}Cl_2N_3O_3Rh$ (582.2503): calcd. C 51.6, H 3.1, N 7.2; found C 51.8, H 2.9, N 7.5.
3c: $C_{31}H_{22}Cl_2N_3O_3Rh$ (658.3479): calcd. C 56.6, H 3.4, N 6.4; found C 56.7, H 3.4, N 6.4.
3d: $C_{27}H_{20}Cl_2N_3O_4Rh$ (624.2871): calcd. C 51.9, H 3.2, N 6.7; found C, 51.6, H 2.9, N 7.0.
4: $C_{20}H_{13}Cl_2N_2O_3Rh$ (503.1491): calcd. C 47.7, H 2.6, N 5.6; found C 47.8, H 2.4, H 5.5.

Pyridyl Ligand Exchange of 3d and 3b: Complex **3d** (6 mg, 0.01 mmol) and $CDCl_3$ (1 cm^3) were placed in an oven-dried NMR tube. A tenfold excess of pyridine was added. After warming the tube in a thermostat at 30 °C for 1 h, ^{1}H NMR spectra were recorded at time intervals of 1 h until no **3d** was detected. After 20 h, all **3d** had been converted into **3b** according to the ^{1}H NMR spectroscopic data. The single metal-containing product of **3b** was obtained by TLC separation with a solvent mixture of *n*-hexane/CH_2Cl_2 (1:10, v/v) as the eluent.

The single metal-containing products **3c** and **3d** were obtained by a similar procedure of ligand exchange with **3d** and **3b** and 4-phenylpyridine and 4-acetylpyridine, respectively.

Reaction Between $[\mathrm{Rh^I(\mu\text{-}Cl)(CO)_2}]_2$ and 1,2-Naphthoquinone-2-oxime: $[\mathrm{Rh^I(\mu\text{-}Cl)(CO)_2}]_2$ (39 mg, 0.1 mmol) and 1,2-naphthoquinone-2-oxime (104 mg, 0.6 mmol) was dissolved in benzene (50 mL) and stirred at room temperature for 3 h. The solvent was removed from the dark red solution and the residue chromatographed by TLC with *n*-hexane/CH_2Cl_2 (1:5, v/v) as the eluent. Three red products were isolated as $[\mathrm{Rh(\eta^2\text{-}nqo)_2(nqi)Cl}]$ (**5**; 10%, 13 mg), *fac*-$[\mathrm{Rh(\eta^2\text{-}nqo)_3}]$ (**6**; 40% yield, 49 mg) and *mer*-$[\mathrm{Rh(\eta^2\text{-}nqo)_3}]$ (**7**; 10% yield, 12 mg). Single crystals of **5** were grown by slow evaporation of a *n*-hexane/CH_2Cl_2 solution at −20 °C.
5: $C_{30}H_{19}ClN_3O_5Rh$ (639.86): calcd. C 56.3, H 3.0, N 6.6; found C 56.0, H 2.7, N 6.6.
6: $C_{30}H_{18}N_3O_6Rh$ (619.40): calcd. C 58.2, H 2.9, N 6.8; found C 58.0, H 2.6, N 6.8.
7: $C_{30}H_{18}N_3O_6Rh$ (619.40): calcd. C 58.2, H 2.9, N 6.8; found C 58.2, H 3.0, N 7.0.

Crystallography:
Single crystals of **1a**, **2b**, **4** and **5** were obtained as described above. A crystal of **1a** was mounted on a glass fibre by means of epoxy resin, while crystals of **2b**, **4** and **5** were sealed in Lindemann glass capillaries. Crystal intensity data were collected for **1a**, **2b** and **4** on

Table 3. Crystal data and data collection parameters for compounds **1a**, **2b**, **4** and **5**

	1a	**2b**	**4**	**5**
Empirical formula	$C_{46}H_{36}Cl_2NO_2P_2Rh$	$C_{26}H_{18}Cl_4N_3O_4Rh$	$C_{21}H_{14}Cl_5N_2O_3Rh$	$C_{34}H_{27}Cl_9N_3O_5Rh$
M	870.55	681.16	622.52	979.59
Crystal colour, habit	Red, block	Red, block	Orange-red, block	Red, block
Crystal dimensions/mm	0.12 × 0.12 × 0.17	0.22 × 0.16 × 0.18	0.24 × 0.26 × 0.31	0.13 × 0.12 × 0.14
Crystal system	Monoclinic	Triclinic	Monoclinic	Monoclinic
Space group	$P2_1/n$ (no. 14)	$P\bar{1}$(no.2)	$P2_1/n$ (no.14)	$P2_1/n$ (no.14)
a/Å	11.506(1)	7.719(2)	9.088(1)	11.883(1)
b/Å	18.713(1)	12.881(2)	17.651(1)	15.026(2)
c/Å	19.574(1)	15.271(3)	15.154(1)	22.833(1)
α/°	−	111.636(3)	−	−
β/°	106.62(2)	91.619(3)	106.22(2)	96.35(1)
γ/°	−	98.801(3)	−	−
U/Å^3	4038.5(6)	1388.8(4)	2334.1(4)	4051.9(6)
Z	4	2	4	4
D_c/g cm^{-3}	1.432	1.629	1.771	1.606
μ(Mo-K_α)/cm^{-1}	6.73	10.35	13.28	10.56
Reflections collected				38432
Unique reflections	9355	6236	5405	3295
Observed reflectons [$I > 1.5\sigma(I)$]	5568	5092	2635	1885
R	0.051	0.058	0.092	0.094
R'	0.047	0.072	0.077	0.098
Goodness of fit, S	1.00	2.51	2.06	2.14

a Siemens Smart CCD and for **5** on a MAR research image-plate scanner, using graphite-monochromated Mo-K_α radiation (λ = 0.71073 Å) for unit-cell determination and data collection. Intensity data were corrected for Lorentz and polarisation effects. An approximation to absorption correction by inter-image scaling was also applied. Summaries of the crystallographic data, structure solution and refinement are given in Table 3. Scattering factors were taken from part a in ref.[47] and anomalous dispersion effects were included in *Fc* (part b). The structures were solved by direct methods (SIR 92[48] for **1a**, **4** and **5**; SHELXS 86[49] for **2b**). The remaining non-hydrogen atoms were determined by subsequent Fourier and Fourier-difference techniques. The structures were refined by full-matrix least-squares analysis on *F*, with all non-hydrogen atoms refined anisotropically until convergence was reached. The hydrogen atoms of the organic moieties were generated in their ideal positions (C−H, 0.95Å). They were included in the structure factor calculations on a Silicon-Graphics computer using the program package TEXSAN.[50]

Crystallographic data (excluding structure factors) for the structures **1a**, **2b**, **4** and **5** reported in this paper have been deposited with the Cambridge Crystallographic Data Centre as supplementary publication no. CCDC-144600 to -144603, respectively. Copies of the data can be obtained free of charge on application to CCDC, 12 Union Road, Cambridge CB2 1EZ, UK [Fax: (internat.) +44-1223/336-033; E-mail: deposit@ccdc.cam.ac.uk].

Acknowledgments

We gratefully acknowledge financial support from the Hong Kong Research Grants Council and the University of Hong Kong. X.-X. Liu acknowledges the receipt of a demonstratorship administered by the Department of Chemistry, University of Hong Kong.

---

[1] U. Kolle, M. Grutzel, *Angew. Chem. Int. Ed. Engl.* **1987**, *26*, 567−570.

[2] H. C.-Y. Bettega, J.-C. Moutet, S. Tingry, *J. Electroanal. Chem.* **1995**, *391*, 51−61.

[3] I. M. F. De Oliveira, J.-C. Moutet, N. Vlachopoulos, *J. Electroanal. Chem.* **1990**, *291*, 243−249.

[4] C. Caix, S. Chardon-Noblat, A. Deronzier, J.-C. Moutet, S. Tingry, *J. Organomet. Chem.* **1997**, *540*, 105−111.

[5] S. Cosnier, A. Deronzier, N. Vlachopoulos, *J. Chem. Soc., Chem. Commun.* **1989**, 1259−1261.

[6] S. Cosnier, H. Gunther, *J. Electroanal. Chem.* **1991**, *315*, 307−312.

[7] R. Ruppert, S. Herrmann, E. Steckhan, *Tetrahedron Lett*. **1987**, *28*, 6583−6586.

[8] B. Foretic, N. Burger, V. Hankonyi, *Polyhedron* **1995**, *14*, 605−609.

[9] J. Charalambous, W. C. Stoten, K. Henrick, *Polyhedron* **1989**, *8*, 103−107.

[10] X.-X. Liu, W.-T. Wong, *Polyhedron* **2000**, *19*, 7−21.

[11] N. Ghatak, S. Bhattacharya, *Transition Met. Chem*. **1996**, *21*, 423−427.

[12] O. K. Borggaard, H. E. M. Christensen, S. P. Lund, *Analyst* **1984**, *109*, 1179−1182.

[13] O. K. Borggaard, H. E. M. Christensen, T. K. Nielsen, M. Willems, *Analyst* **1982**, *107*, 1479−1483.

[14] H. Barjesteh, E. G. Brain, J. Charalambous, P. Gaganatsou, T. A. Thomas, *J. Chem. Res. (S)* **1995**, 454−454.

[15] A. McKillop, T. S. B. Sayer, *J. Org. Chem.* **1976**, *41*, 1079−1080.

[16] R. G. Buckley, J. Charalambous, M. J. Kensett, M. McPartlin, D. Mukerjee, E. G. Brain, J. M. Jenkins, *J. Chem. Soc., Perkin Trans. 1* **1983**, 693−697.

[17] R. G. Buckley, J. Charalambous, E. G. Brain, *J. Chem. Soc., Perkin Trans. 1* **1982**, 1075−1078.

[18] J. Charalambous, L. I. B. Haines, J. S. Morgan, D. S. Peat, M. J. M. Champbell, J. Bailey, *Polyhedron* **1987**, *6*, 1027−1032.

[19] H. Saarinen, J. Korvenranta, *Acta Chem. Scand.* **1975**, *A29*, 409−413.

[20] J. Korvenranta, H. Saarinen, *Acta Chem. Scand.* **1975**, *A29*, 861−865.

[21] J. Charalambous, K. Henrick, Y. Musa, R. G. Rees, R. N. Whiteley, *Polyhedron* **1987**, *6*, 1509−1512.

[22] A. K. Das, A. Rueda, L. R. Falvello, S.− M. Peng, S. Bhattacharya, *Inorg. Chem*. **1999**, *38*, 4365−4368.

[23] K. K.-H. Lee, W.-T. Wong, *J. Chem. Soc., Dalton Trans.* **1997**, 2987−2995.

[24] K. K.-H. Lee, W.-T. Wong, *J. Organomet. Chem.* **1997**, *547*, 329−335.

[25] X.-X. Liu, W.-T. Wong, *Inorg. Chim. Acta*. **2000**, *299*, 16−27.

[26] R. Dreos, G. Tauzher, S. Geremia, L. Randaccio, F. Asaro, G. Pellizer, C. Tavagnacco, G. Costa, *Inorg. Chem.* **1994**, *33*, 5404−5410.

[27] H. C.-Y. Bettega, J.-C. Moutet, *J. Electroanal. Chem.* **1994**, *364*, 271−275.

[28] I. M. F. De Oliveira, J.-C. Moutet, *J. Electroanal. Chem.* **1993**, *361*, 203−210.

[29] G. Kew, K. DeArmond, K. Hanck, *J. Phys. Chem*. **1974**, *78*, 727−734.

[30] M. Ladwig, W. Kaim, *J. Organomet. Chem.* **1991**, *419*, 233−243.

[31] S. Chardon-Noblat, S. Cosnier, A. Deronzier, N. Vlachopoulos, *J. Electroanal. Chem.* **1993**, *352*, 213−228.

[32] U. Kolle, B.-S. Kang, P. Infelta, P. Comte, M. Gratzel, *Chem. Ber*. **1989**, *122*, 1869−1880.

[33] B. Soucaze-Guillous, H. Lund, *Acta Chem. Scand*. **1998**, *52*, 417−424.

[34] S. Djebbar-Sid, O. Benali-Baitich, J. P. Deloume, *Polyhedron* **1997**, *16*, 2175−2182.

[35] W. Kaim, R. Reinhardt, M. Sieger, *Inorg. Chem*. **1994**, *33*, 4453−4459.

[36] P. C. Christidis, A. Dodd, N. D. Pathirana, J. Charalambous, M. McPartlin, N. Talee, *Acta Cryst*. **1991**, C*47*, 2640−2642.

[37] K. E. Linder, D. P. Nowotnik, M. F. Malley, J. Z. Gougoutas, A. D. Nunn, *Inorg. Chim. Acta* **1991**, *190*, 249−255.

[38] D. Steinborn, M. Rausch, C. Bruhn, *J. Organomet. Chem.* **1998**, *561*, 191−197.

[39] P. W. Carreck, J. Charalambous, M. J. Kensett, M. McPartlin, R. Sims, *Inorg. Nucl. Chem. Lett*. **1974**, *10*, 749−751.

[40] S. Candeloro, D. Grdenic, N. Taylor, B. Thompson, M. Viswamitra, D. C. Hodgkin, *Nature* **1969**, *224*, 589−591.

[41] P. Basu, S. B. Choudhury, S. Pal, A. Chakravorty, *Inorg. Chem.* **1989**, *28*, 2680−2686.

[42] P. Basu, S. Pal, A. Chakravorty, *J. Chem. Soc., Chem. Commun.* **1989**, 977−978.

[43] P. Basu, A. Chakravorty, *J. Chem. Soc., Chem. Commun.* **1992**, 809−810.

[44] D. Ray, A. Chakravorty, *Inorg. Chem.* **1988**, *27*, 3292−3297.

[45] K. C. Kalia, A. Chakravorty, *Inorg. Chem.* **1969**, *8*, 2586−2590.

[46] K. C. Kalia, A. Chakravorty, *Inorg. Chem.* **1968**, *7*, 2016−2020.

[47] D. T. Cromer, J. T. Waber, *International Tables for X-ray Crystallography*, Kynoch Press, Birmingham, **1974**, Vol. 4; (a) Table 2.2.B; (b) Table 2.3.1.

[48] SIR 92, A. Altomare, M. C. Burla, M. Camalli, M. Cascarano, C. Giacovazzo, A. Guagliardi, G. Polidori, *J. Appl. Crystallogr.* **1994**, *27*, 435−442.

[49] G. M. Sheldrick, in *Crystallographic Computing 3*, G. M. Sheldrick, C. Kruger, R. Goddard, Eds., Oxford University Press, **1985**, 175−189.

[50] TEXSAN, Crystal Structure Analysis Package, Molecular Structure Corporation, Houston, TX, **1985** and **1992**.

Received May 24, 2000
[I00215]